Technical Notes

Uncertainty Quantification in State-Specific Modeling of Thermal Relaxation and Dissociation of Oxygen

Xiaoyong Wang,* Qizhen Hong,† Chao Yang,‡
and Quanhua Sun§
*Chinese Academy of Science, 100190 Beijing,
People's Republic of China*

https://doi.org/10.2514/1.J062555

I. Introduction

THE high temperatures in hypersonic flows induce many complicated physical and chemical processes, such as vibrational and electronic energy excitation, dissociation of molecules, and even ionization [1,2]. Thermochemical nonequilibrium phenomena are ubiquitous in hypersonic flows [1–3]. Developing reliable and accurate computational tools to predict these thermochemical nonequilibrium flows is essential for designing hypersonic vehicles [1–3].

Nowadays, two typical models, i.e., the two-temperature and state-to-state (StS) models, have been proposed to simulate the thermochemical nonequilibrium flows [3]. Due to the simpleness, the two-temperature model is widely used and implemented in well-known CFD codes [4–6]. In the two-temperature model, each internal energy mode is assumed to follow a Boltzmann distribution corresponding to its equilibrium temperature. Therefore, its applicability is only limited to the flow where vibrational distribution slightly deviates from equilibrium [3]. Furthermore, the reaction rate constants utilized in the two-temperature model are based primarily on the decades-old shock-tube data [7], which includes significant uncertainties.

Based on the recent advances in computational chemistry, the StS model has been developed to overcome the deficiencies of the two-temperature model [8]. The StS model treats each internal energy state as a pseudospecies and directly tracks the states' population [8]. Consequently, the assumption of Boltzmann distribution is abandoned. However, the StS model requires numerous rates for all the excitation and dissociation processes from each internal energy state [9]. These rates are usually obtained by the quantum-classical method, quasi-classical trajectory (QCT) calculations, or approximate models, including Landau–Teller model, Schwartz–Slawsky–Herzfeld (SSH) theory, and forced harmonic oscillator (FHO) model [3,9]. On the whole, due to hundreds of internal energy states and kinetic processes to be considered, the computing consumption of the StS model is vast, restricting its application only to simplified zero- or one-dimensional cases [3,10,11].

Another issue for the StS model to be noted is the uncertainties in the excitation and dissociation rates. Baluckram and Andrienko state that up to three-orders-of-magnitude uncertainties are observed between the FHO model and QCT for bound–bound rates of the higher-lying states because of the harmonicity and nonreactive assumptions [11]. Furthermore, nearly one-order-of-magnitude uncertainty is observed from the QCT databases proposed by different authors for the state-specific dissociation rates [11]. StS results are well known to be sensitive to the excitation and dissociation rates employed. Therefore, the uncertainty quantification of the StS model should be assessed.

In this study, we perform Monte Carlo uncertainty and sensitivity analysis in state-specific modeling of thermal relaxation and dissociation of oxygen behind a normal shock. The vibrational temperature and the mole fraction of O are chosen as the output quantities of interests (QoIs). The excitation and dissociation rates are considered as uncertain parameters.

II. State-to-State Method

In this paper, the thermal relaxation and dissociation of O_2 behind normal shock are calculated by StS. The freestream conditions are set according to the shock tube experiments conducted by Ibraguimova et al., i.e., $V = 4440$ m/s, $P = 0.8$ Torr, and $T = 295$ K [12]. The governing equations for the flow behind normal shock wave can be expressed as [10,13]

$$\frac{\partial}{\partial x}\begin{pmatrix} \rho_{O_2(i)}u \\ \rho_O u \\ \rho u^2 + p \\ \rho u(h + u^2/2) \end{pmatrix} = \begin{pmatrix} \omega_{O_2(i)} \\ \omega_O \\ 0 \\ 0 \end{pmatrix} \quad (1)$$

where ρ_O and $\rho_{O_2(i)}$ denote the densities of O and O_2 at ith vibrational level; u, p, and h are the velocity, pressure, and enthalpy, respectively; and $\omega_{O_2(i)}$ and ω_O are the mass production rates of O_2 at ith vibrational level and O, respectively.

The mass production rates of O_2 at ith vibrational level are expressed as [10,13]

$$\frac{N_A}{M_{O_2}}\omega_{O_2(i)} = \sum_{f \neq i}\{k_{V-T}(f \to i)[O_2(f)][O] - k_{V-T}(i \to f)[O_2(i)][O]\}$$
$$+ \sum_{i_2}\sum_{f_1}\sum_{f_2}\{k_{V-V-T}(f_1, f_2 \to i, i_2)[O_2(f_1)][O_2(f_2)]$$
$$- k_{V-V-T}(i, i_2 \to f_1, f_2)[O_2(i)][O_2(i_2)]\}$$
$$+ k_{rec}^{O_2}(i)[O_2][O]^2 - k_{dis}^{O_2}(i)[O_2(i)][O_2] + k_{rec}^{O}(i)[O]^3$$
$$- k_{dis}^{O}(i)[O_2(i)][O] \quad (2)$$

where N_A is the Avogadro constant; M_s is the species molecular mass; k_{V-T} and k_{V-V-T} are the vibration–translation (V-T) rate and vibration–vibration–translation (V-V-T) rate, respectively; $k_{dis}^{O_2}$ and $k_{rec}^{O_2}$ are the vibration–dissociation (V-D) and recombination rates for O_2–O_2 collision; and k_{dis}^{O} and k_{rec}^{O} are the V-D and recombination rates for O_2–O collision.

The mass production rates of O are expressed as [10,13]

$$\frac{N_A}{M_O}\omega_O = 2\sum_i \left\{ k_{\mathrm{dis}}^{O_2}[O_2(i)][O_2] - k_{\mathrm{rec}}^{O_2}[O_2][O]^2 + k_{\mathrm{dis}}^{O}[O_2(i)][O] \right.$$
$$\left. - k_{\mathrm{rec}}^{O}[O]^3 \right\} \tag{3}$$

In the current study, 47 vibrational states of O_2 in the ground electronic state are considered [14,15]. The V-V-T bound–bound transition rates are computed by FHO model [16]. The V-T and state-specific dissociation rates are obtained from the QCT database proposed by Andrienko and Boyd [14,15,17]. The V-T rates and V-D rates for O_2–O_2 and O_2–O collision proposed by Andrienko et al. are presented in references [14,15,17]. In this study, the multiquantum V-V-T transitions with jumps larger than 5 are neglected [16].

The above stiff equations are conducted from a shock wave reference frame, and solved by second-order additive semi-implicit Runge–Kutta method [18]. The simulations are performed on a uniform grid of 20,000 nodes totally covering 2 cm in distance behind the shock. The initial conditions are derived from the Rankine–Hugoniot relations [13].

III. Uncertainty Quantification Approach

Monte Carlo sensitivity and uncertainty analysis have already been successfully utilized to identify the primary source of uncertainty in chemical kinetic models [19,20]. Therefore, Monte Carlo uncertainty and sensitivity analysis perform the uncertainties analysis in state-specific modeling of thermal relaxation and dissociation of oxygen behind a normal shock. The main steps are briefly outlined as follows:

1) It is well known that StS models consider hundreds and thousands of kinetic processes between the states. However, significant uncertainty still exists in the rates of these kinetic processes. In this study, all the rates of the StS modeling of thermal relaxation and dissociation of O_2 behind normal shock are treated as uncertainty inputs. Totally, 61,263 rates, including 47 V-D and 60,088 V-V-T rates for O_2–O_2 collision and 47 V-D and 1081 V-T rates for O_2–O collision [11,14,15,17], are identified as varying input parameters redefining as [19]

$$P = \log_{10}\left(\frac{k}{k^0}\right) \tag{4}$$

where k and k^0 are the varying rate and baseline rate, respectively.

2) The identified input parameters P are statistically varying, representing their typical uncertainties. Each input parameter varies independently with a Gaussian distribution. The mean value and standard deviation of the Gaussian distribution are set to 0 and 0.5, respectively, which means that the probability of this parameter varying between an order of magnitude is 95.4% [19].

3) The randomly varying parameters are input in the StS modeling, and many StS runs are conducted to obtain the corresponding QoIs.

4) Correction coefficients are obtained for each input–output pair, and the uncertainty contributions to the QoIs are identified and ranked.

IV. Results

A. Statistical Convergence

In this work, 5000, 10,000, and 15,000 runs are made to ensure statistical accuracy. Figure 1 shows the mean value and standard deviation of vibrational temperature profiles. Figure 2 shows the mean value and standard deviation of mass fraction for O after the shock. Compared with the results of 10,000 samples, increasing the number of samples has little effect on the predicted mean value and standard deviation of mole fraction of O and temperature profiles after the shock. Therefore, 10,000 samples are enough to get statistical convergence results and evaluate the following uncertainty study.
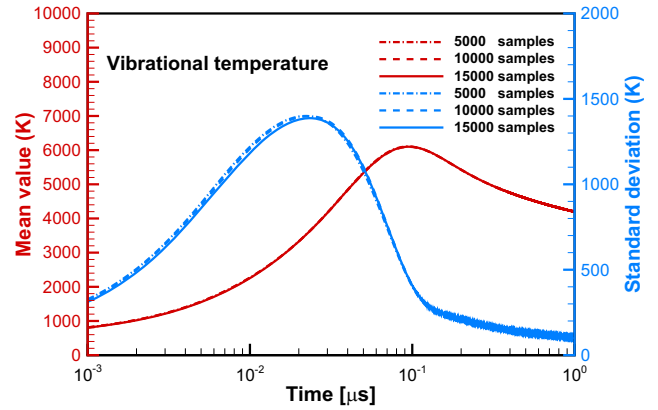

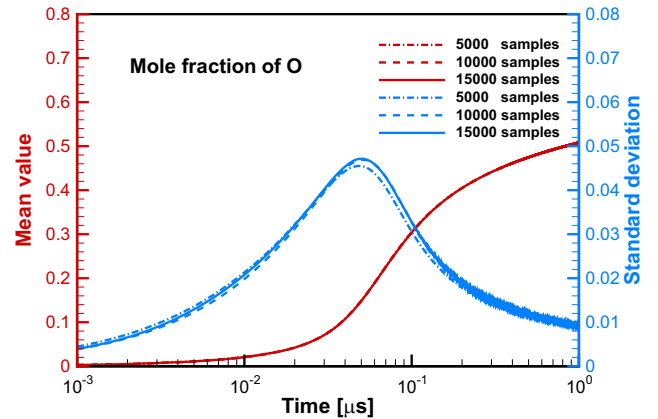**Fig. 1 Vibrational temperature.**

Fig. 2 Mole fraction of O.

B. Uncertainty Analysis

Figure 3 shows the profiles of vibrational temperature. The mean, maximum, and minimum values evaluated by 10,000 samples are compared with baseline results, experimental data [12], and other StS results [10,11]. Compared with the baseline result, the mean value is slightly higher before 0.1 μm, and lower afterward. Overall, the mean value of vibrational temperature agrees well with experiments and baseline results. However, the uncertainty in rates induces considerable uncertainty in vibrational temperature, especially before 0.1 μm. The maximum interval between the maximum and minimum vibrational temperature simultaneously is nearly 10,000 K. After 0.1 μm, the gap between the maximum and minimum vibrational temperature is gradually decreased.
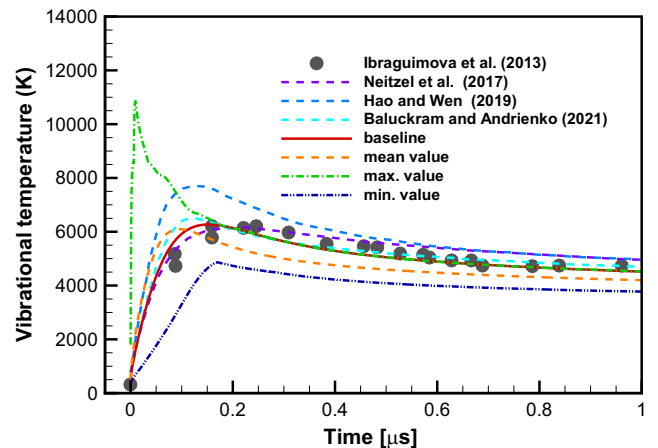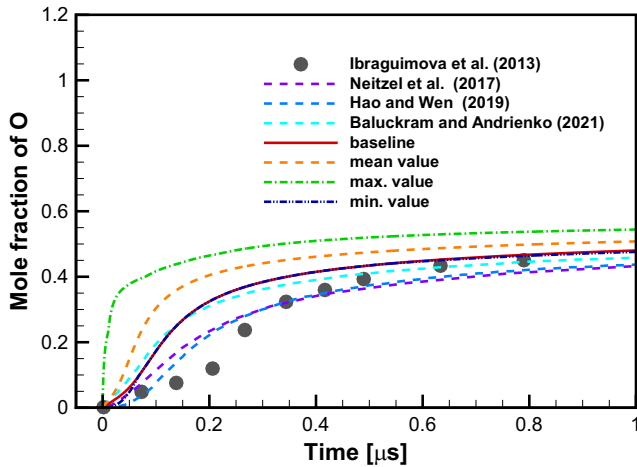

Fig. 3 Uncertainty of vibrational temperature.

Fig. 4   Uncertainty of mole fraction of O.

Fig. 5   Sensitivities for vibrational temperature.

Fig. 6   Sensitivities for mole fraction of O.

Figure 4 shows the profiles of the mole fraction of O. The mean value of the mole fraction of O is slightly higher than the baseline value, which is significantly different from the experiments before 0.4 μm and agrees well with experiments after 0.4 μm. The uncertainty in rates also induces considerable uncertainty in the mole fraction of O, especially before 0.2 μm. Same as the vibrational temperature profiles, the interval between the maximum and minimum value of the mole fraction of O is comparably small after 0.2 μm and large before 0.2 μm.

In comparison, the baseline results of vibrational temperature and mole fraction of O agree well with the results of Baluckram and Andrienko [11], which are also consistent with the experiments [12]. The bound–bound (V-T) and bound–free (V-D) rate coefficients used in this paper are mainly taken from the Andrienko et al. database presented in detail in references [14,15,17]. Therefore, the results of this paper are consistent with Baluckram and Andrienko [11]. However, the results of Neitzel et al. [13] and Hao and Wen [10] lie without the maximum and minimum results of this study. We can probably infer that at least one order of magnitude of uncertainty exists in their rates. Note that the $O_2 - O$ V-T and V-D rates of Neitzel et al. and Hao and Wen are both obtained from the QCT method of Andrienko and Boyd [10,13]. However, Baluckram and Andrienko recently stated that up to one-order-of-magnitude uncertainty exists in the bound–free rates due to the different potential energy surface (PES) used [11].

C.   Sensitivity Analysis

In this section, the square of the correction coefficient is employed to rank the relative contribution of each kinetic rate to the total uncertainty. The correction coefficient $\rho(X, Y)$ of input parameters X and QoIs Y is defined as [21]

$$\rho(X, Y) = \frac{\text{Cov}(X, Y)}{\sqrt{\text{Var}[X]\text{Var}[Y]}} \qquad (5)$$

where $\text{Var}[\cdot]$ is the variance, and $\text{Cov}(X, Y)$ is covariance defined as

$$\text{Cov}(X, Y) = E(XY) - E(X)E(Y) \qquad (6)$$

where $E[\cdot]$ is the mean value.

The previous study shows that the uncertainties in rates induce significant uncertainties in vibrational temperature. Therefore, the maximum vibrational temperature and mole fraction of O at maximum vibrational temperature are chosen as the QoIs. We prioritize the kinetic rates according to their contributions to the uncertainty in QoIs. The sensitivities of QoIs are quantified in Figs. 5 and 6, respectively. The maximum correction coefficient normalizes the correction coefficient of each reaction. A high correction coefficient suggests that the reaction or rate strongly affects the QoIs [21].

For the maximum vibrational temperature, $O_2(0) + O_2(0) \rightleftharpoons O_2(0) + O_2(1)$ (V-T energy transfer), $O_2(0) + O_2 \rightleftharpoons O + O + O_2$,
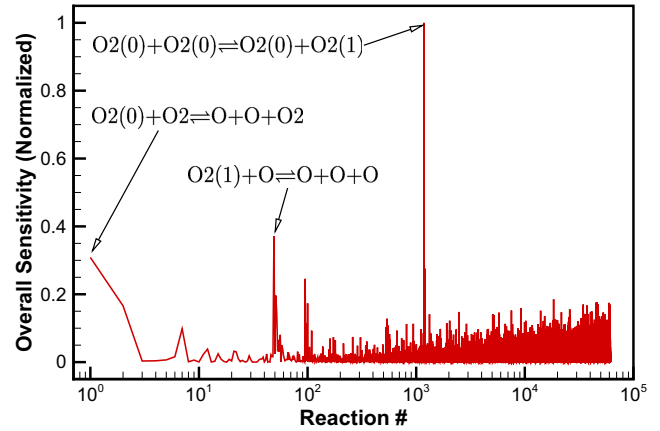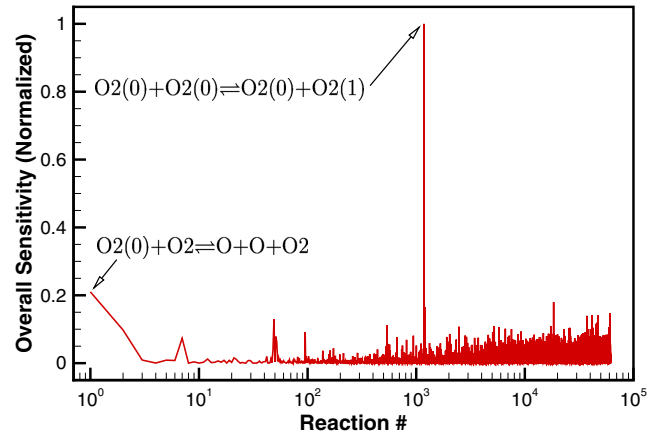
and $O_2(1) + O \rightleftharpoons O + O + O$ are the primary reactions. For the mole fraction of O at maximum vibrational temperature, $O_2(0) + O_2(0) \rightleftharpoons O_2(0) + O_2(1)$ and $O_2(0) + O_2 \rightleftharpoons O + O + O_2$ are the dominant reactions. This is because large number of O_2 have not dissociated and are in the ground state at maximum vibrational temperature. In addition, the vibration temperature in this paper is defined as the number density ratio of first excited state to the ground state [3], i.e.,

$$Tv = \frac{e_v(1) - e_v(0)}{k_B \ln([O_2(1)]/[O_2(0)])} \qquad (7)$$

Therefore, the number density changes of the ground and first excited states can significantly affect the vibrational temperature. Furthermore, recent QCT and FHO databases consistently show that the V-T rates at low-lying states are faster than V-V-T at high-temperature conditions [11]. Due to the above reasons, $O_2(0) + O_2(0) \rightleftharpoons O_2(0) + O_2(1)$ dominantly determines the vibrational temperature and mole fraction of O behind the shock. Although the dissociation rates of low-lying vibrational states are lower than those of the higher states [11], $O_2(0) + O_2 \rightleftharpoons O + O + O_2$ is more important because a large number of O_2 are in the ground state.

In the end, we solely speed up or slow down the rates of $O_2(0) + O_2(0) \rightleftharpoons O_2(0) + O_2(1)$ or $O_2(0) + O_2 \rightleftharpoons O + O + O_2$ by an order of magnitude, and four additional StS runs are performed to verify the above conclusion. The results are shown in Figs. 7 and 8. Figure 7a shows that changing the rate of $O_2(0) + O_2(0) \rightleftharpoons O_2(0) + O_2(1)$ significantly affects the vibrational temperature profiles before 0.2 μm. However, no discrepancy is found after 0.2 μm. Note that the sensitivity analysis is performed only for the maximum vibrational temperature. Therefore we only analyze the data before 0.2 μm. In
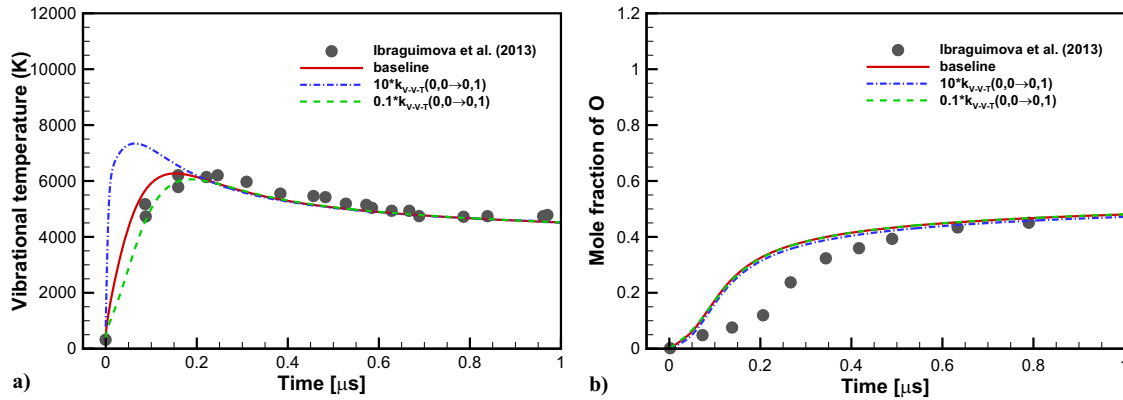
Fig. 7   Effect of $O_2(0) + O_2(0) \rightleftharpoons O_2(0) + O_2(1)$. a) Vibrational temperature; b) mole fraction of O.
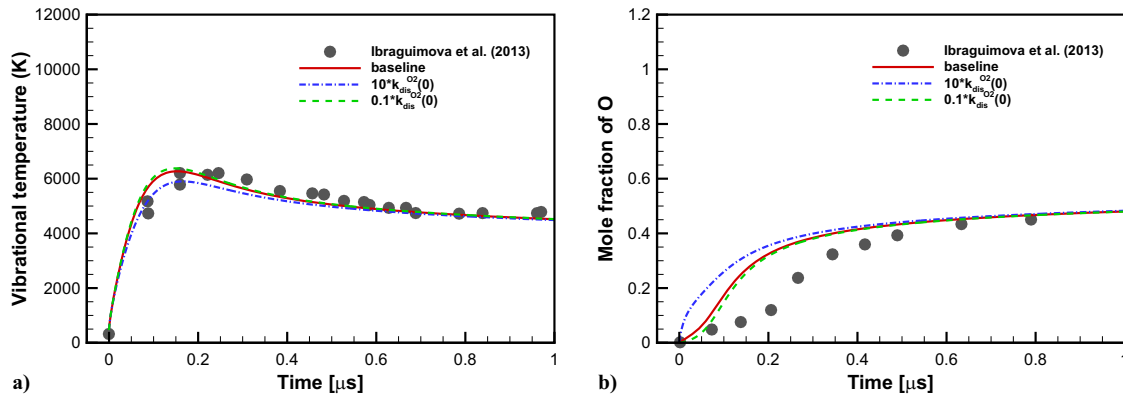

Fig. 8   Effect of $O_2(0) + O_2 \rightleftharpoons O + O + O_2$. a) Vibrational temperature; b) mole fraction of O.

comparison, Fig. 8a shows that the effect of $O_2(0) + O_2 \rightleftharpoons O + O + O_2$ on vibrational temperature is relatively weak. Nevertheless, the apparent difference still can be observed. The effect of $O_2(0) + O_2 \rightleftharpoons O + O + O_2$ on the mole fraction of O is visible in Fig. 8b. However, Fig. 7b shows that $O_2(0) + O_2(0) \rightleftharpoons O_2(0) + O_2(1)$, which is quantified as a primary rate in Fig. 6, does not affect the mole fraction of O. We can infer that the rate mentioned above first affects the number density of ground state of O_2, then through the reaction of $O_2(0) + O_2 \rightleftharpoons O + O + O_2$, finally affects the mole fraction of O. In general, the effects of the above two reactions on the vibrational temperature and mole fraction of O are fairly significant.

V.   Conclusions

Monte Carlo uncertainty and sensitivity analysis perform the uncertainties analysis in the StS modeling of thermal relaxation and dissociation of oxygen behind a normal shock. The 61,263 excitation and dissociation rates are considered as uncertain parameters statistically varying between an order of magnitude. The maximum vibrational temperature and the mole fraction of O at maximum vibrational temperature are chosen as the QoIs. 10,000 runs are used to get statistical convergence results. The results show that the uncertainty in V-T and V-V-T rates imposes a noticeable effect on the QoIs. $O_2(0) + O_2(0) \rightleftharpoons O_2(0) + O_2(1)$ and $O_2(0) + O_2 \rightleftharpoons O + O + O_2$ are identified as the dominant reactions that affect the QoIs significantly. This study also infers that more accurate rates for the StS model are still needed, and we can focus on the rates of $O_2(0) + O_2(0) \rightleftharpoons O_2(0) + O_2(1)$ and $O_2(0) + O_2 \rightleftharpoons O + O + O_2$.

Acknowledgments

References

[1] Candler, G. V., "Rate Effects in Hypersonic Flows," *Annual Review of Fluid Mechanics*, Vol. 51, No. 1, 2019, pp. 379–402.
https://doi.org/10.1146/annurev-fluid-010518-040258

[2] Gnoffo, P. A., "Planetary-Entry Gas Dynamics," *Annual Review of Fluid Mechanics*, Vol. 31, No. 1, 1999, pp. 459–494.
https://doi.org/10.1146/annurev.fluid.31.1.459

[3] Hong, Q., Wang, X., Hu, Y., and Sun, Q., "Development of a Stagnation Streamline Model for Thermochemical Nonequilibrium Flow," *Physics of Fluids*, Vol. 32, No. 4, 2020, Paper 046102.
https://doi.org/10.1063/5.0003247

[4] Nompelis, I., and Candler, G. V., "US3D Predictions of Double-Cone and Hollow Cylinder-Flare Flows at High-Enthalpy (Invited)," *44th AIAA Fluid Dynamics Conference*, AIAA Paper 2014-3366, 2014.
https://doi.org/10.2514/6.2014-3366

[5] Holloway, M. E., Chaudhry, R. S., and Boyd, I. D., "Assessment of Hypersonic Double-Cone Experiments for Validation of Thermochemistry Models," *Journal of Spacecraft and Rockets*, Vol. 59, No. 2, 2022, pp. 389–400.
https://doi.org/10.2514/1.A35052

[6] Hao, J., Wang, J., and Lee, C., "Assessment of Vibration–Dissociation Coupling Models for Hypersonic Nonequilibrium Simulations," *Aerospace Science and Technology*, Vol. 67, Aug. 2017, pp. 433–442, https://www.sciencedirect.com/science/article/pii/S1270963816313608.
https://doi.org/10.1016/j.ast.2017.04.027

[7] Chaudhry, R. S., Boyd, I. D., Torres, E., Schwartzentruber, T. E., and Candler, G. V., "Implementation of a Chemical Kinetics Model for Hypersonic Flows in Air for High-Performance CFD," *AIAA Scitech 2020 Forum*, AIAA Paper 2020-2191, 2020.
https://doi.org/10.2514/6.2020-2191

[8] Nagnibeda, E., and Kustova, E., *Non-Equilibrium Reacting Gas Flows: Kinetic Theory of Transport and Relaxation Processes*, Springer Science & Business Media, Berlin, 2009, Chap. 2.

[9] Jo, S. M., Venturi, S., Munafò, A., Priyadarshini, M. S., and Panesi, M., "Physics-Driven Modeling for Aerothermodynamics," *AIAA Aviation 2021 Forum*, AIAA Paper 2019-3143, 2021.
https://doi.org/10.2514/6.2021-3143

[10] Hao, J., and Wen, C.-Y., "Maximum Entropy Modeling of Oxygen Vibrational Excitation and Dissociation," *Physical Review Fluids*, Vol. 4, No. 5, 2019, Paper 053401.
https://doi.org/10.1103/PhysRevFluids.4.053401

[11] Baluckram, V. T., and Andrienko, D., "First-Principle Simulation of Vibrational Activation and Dissociation in Oxygen Shock Flows," *AIAA Scitech 2021 Forum*, AIAA Paper 2021-0447, 2021.
https://doi.org/10.2514/6.2021-0447

[12] Ibraguimova, L. B., Sergievskaya, A. L., Levashov, V. Y., Shatalov, O. P., Tunik, Y. V., and Zabelinskii, I. E., "Investigation of Oxygen Dissociation and Vibrational Relaxation at Temperatures 4000–10800 K," *Journal of Chemical Physics*, Vol. 139, No. 3, 2013, Paper 034317.
https://doi.org/10.1063/1.4813070

[13] Neitzel, K., Andrienko, D., and Boyd, I. D., "Aerothermochemical Nonequilibrium Modeling for Oxygen Flows," *Journal of Thermophysics and Heat Transfer*, Vol. 31, No. 3, 2017, pp. 634–645.
https://doi.org/10.2514/1.T4962

[14] Andrienko, D., and Boyd, I. D., "Vibrational Relaxation and Dissociation of Oxygen in Molecule-Atom Collisions," *45th AIAA Thermophysics Conference*, AIAA Paper 2015-3251, 2015.
https://doi.org/10.2514/6.2015-3251

[15] Andrienko, D. A., and Boyd, I. D., "State-Specific Dissociation in O_2–O_2 Collisions by Quasiclassical Trajectory Method," *Chemical Physics*, Vol. 491, July 2017, pp. 74–81, https://www.science direct.com/science/article/pii/S0301010417301842.
https://doi.org/10.1016/j.chemphys.2017.05.005

[16] Hao, J., Wang, J., and Lee, C., "State-Specific Simulation of Oxygen Vibrational Excitation and Dissociation Behind a Normal Shock," *Chemical Physics Letters*, Vol. 681, Aug. 2017, pp. 69–74, https://www.sciencedirect.com/science/article/pii/S0009261417304803.
https://doi.org/10.1016/j.cplett.2017.05.042

[17] Andrienko, D. A., and Boyd, I. D., "Master Equation Study of Vibrational and Rotational Relaxations of Oxygen," *Journal of Thermophysics and Heat Transfer*, Vol. 30, No. 3, 2016, pp. 533–552.
https://doi.org/10.2514/1.T4769

[18] Zhong, X., "Additive Semi-Implicit Runge–Kutta Methods for Computing High-Speed Nonequilibrium Reactive Flows," *Journal of Computational Physics*, Vol. 128, No. 1, 1996, pp. 19–31, https://www.sciencedirect.com/science/article/pii/S002199919690193X.
https://doi.org/10.1006/jcph.1996.0193

[19] Bose, D., Wright, M., and Gokcen, T., "Uncertainty and Sensitivity Analysis of Thermochemical Modeling for Titan Atmospheric Entry," *37th AIAA Thermophysics Conference*, AIAA Paper 2004-2455, 2004.
https://doi.org/10.2514/6.2004-2455

[20] Bose, D., Wright, M. J., and Palmer, G. E., "Uncertainty Analysis of Laminar Aeroheating Predictions for Mars Entries," *Journal of Thermophysics and Heat Transfer*, Vol. 20, No. 4, 2006, pp. 652–662.
https://doi.org/10.2514/1.20993

[21] Venturi, S., Jaffe, R. L., and Panesi, M., "Bayesian Machine Learning Approach to the Quantification of Uncertainties on Ab Initio Potential Energy Surfaces," *Journal of Physical Chemistry A*, Vol. 124, No. 25, 2020, pp. 5129–5146.
https://doi.org/10.1021/acs.jpca.0c02395

D. Livescu
Associate Editor